



Structural neuroimaging findings in migraine patients with restless legs syndrome

Arzu Aldemir¹ · Kaan Yucel² · Hayat Güven³ · Burcu Kamaşak⁴ · Alper Dilli⁵ · Niyazi Acer⁶ · Selçuk Çomoğlu³

Received: 31 January 2020 / Accepted: 28 April 2020 / Published online: 2 June 2020
© Springer-Verlag GmbH Germany, part of Springer Nature 2020

Abstract

Purpose One out of three migraine patients might have accompanying restless legs syndrome (RLS). In our study, we aimed to compare the volumes of the brain structures of migraineurs with and without RLS.

Methods We had 37 female patients with migraine and 17 females as the control group. Nineteen migraineurs had no RLS (RLS₀) and 18 migraineurs had comorbidity of RLS (RLS₁). The volumes of the brain structures were obtained by manual measurements, volBrain, and voxel-based morphometry (VBM). Manually, we measured caudate and putamen volumes. We used age, years of education, depression, anxiety scores, and total intracranial volume as covariates.

Results According to VBM analyses, the volumes of the left superior occipital gyrus and precuneus were increased, and the substantia nigra and cuneus were decreased in the RLS₁ group compared with the RLS₀ group. RLS₁ patients had larger superior temporal gyrus, Brodmann area 38, and left insula, and RLS₀ patients had larger Brodmann area 22, right superior temporal gyrus, and Heschl gyrus compared with controls. Migraine and RLS₀ patients had a smaller corpus callosum anteriorly, whereas RLS₁ patients had a smaller splenium. Caudate volumes were larger in migraine patients via the three techniques. There was a positive relation between the caudate and putamen volumes and attack frequency.

Conclusions Comorbidity of RLS might be a confounding factor in structural neuroimaging studies in migraine. Deficits in the visual network seem to be related to accompanying RLS; deficits in the auditory network are particularly related to migraine.

Keywords Voxel-based morphometry · Migraine · Volumetric magnetic resonance imaging · Restless legs syndrome · Comorbidity

Introduction

Migraine is a common primary headache characterized by throbbing severe pain with a series of several symptoms such

as yawning, fatigue, sensitivity to light, sound, and odor [1]. Migraine has a prevalence of 15%, and almost one-third to one-half of all patients, predominantly females, consulted by neurologists have migraine [2–3]. Along with low back pain, migraine is the main cause of years with disability, constituting 64% of the total cost for headache disorders in Europe [4–5]. One of the reasons that make migraine a complex disorder is the long list of comorbidities. In addition to migraine, patients might have stroke, anxiety, depression, epilepsy, irritable bowel syndrome, pain disorders, and restless legs syndrome (RLS) which probably shares common pathophysiology with migraine [6].

RLS is characterized by an uncomfortable sensation at rest or close to bedtime, particularly in the lower extremities [7]. The prevalence of RLS ranges between 6 and 12% in the general population [8]. One out of three migraineurs might have accompanying RLS [9]. The pathogenesis underlying this comorbidity has not been revealed yet; however, common genetic predisposition [10] and iron accumulation in the brain

✉ Kaan Yucel
sefikkanyucel@aksaray.edu.tr; kaanyucel2014@gmail.com

¹ Department of Neurology, Acıbadem Hospital, Eskişehir, Turkey

² Department of Anatomy, Aksaray University Medical School, Aksaray, Turkey

³ Department of Neurology, Dışkapı Yıldırım Beyazıt Training and Research Hospital, University of Health Sciences, Ankara, Turkey

⁴ Department of Anatomy, Ahi Evran University Medical School, Kırşehir, Turkey

⁵ Department of Radiology, Dışkapı Yıldırım Beyazıt Training and Research Hospital, University of Health Sciences, Ankara, Turkey

⁶ Department of Anatomy, Erciyes University Medical School, Kayseri, Turkey

resulting in defects in the dopaminergic system [11] are among the most popular hypotheses.

In meta-analyses of voxel-based morphometry (VBM) studies on migraine, gray matter volume (GMV) reductions were reported in a variety of structures such as the middle and inferior frontal cortex [12], posterior insular-opercular regions, prefrontal cortex, anterior cingulate cortex [13], lateral inferior frontal gyri, right precentral gyrus, left middle frontal gyrus, and left cingulate gyrus [14]. When it comes to RLS, there have been several studies reporting no volume changes relative to controls [15–18]. On the other hand, volume increases in the pulvinar bilaterally, hippocampus, and middle orbitofrontal gyrus, and decreases in volumes of the bilateral primary somatosensory cortex, left primary motor area, parietal lobes, medial frontal areas, and cerebellum have been reported [19]. Headache and sleep disorders such as RLS have a common neurophysiological and neuroanatomical background with shared chemical and neuroanatomical processes in the pathophysiology. Dysfunction in the dopaminergic system has been postulated as an underlying mechanism for both migraine and RLS [20].

Comorbidities with migraine might be confounding factors for the heterogeneity in volumetric findings. There has been only one volumetric study where the brains of migraineurs with and without comorbid RLS were compared with patients with RLS and a control group [21]. Yang et al. [21] found changed GMV in the right medial frontal gyrus in migraineurs with RLS compared with the control group, which also correlated with sleep quality. In another study, Yang et al. [22] also reported changes in the functional connectivity in attentional nociceptive control and sensory-related networks between the migraineurs with and without RLS.

In this study, we compared volumetric measurements among migraineurs with and without RLS and controls by using three techniques: manual stereological measurements of the caudate and putamen, volBrain, and VBM. Based on the “dopaminergic link” hypothesis, we sought to investigate whether the basal ganglia, besides other brain structures, would be affected by RLS as a comorbidity of migraine.

Methods

Participants

The study included 37 right-handed females who were diagnosed as having migraine according to the International Classification of Headache Disorders (ICHD) criteria [23] and 17 healthy right-handed female volunteers as a control group. The patient group was divided into two subgroups: 19 migraineurs with no RLS (RLS₀) and 18 migraineurs with comorbid RLS (RLS₁). Subjects with a history of chronic pain,

systemic diseases, and psychiatric diseases were excluded from the study. The control group was evaluated for the presence of RLS and headache according to diagnostic criteria and subjects diagnosed with any of them were not included. Patients had no history of neurological disorder other than migraine or RLS and medication except non-steroidal anti-inflammatory drugs, paracetamol, and acetylsalicylic acid. Patients who had a headache within the last 72 h prior to the magnetic resonance imaging (MRI) scan were also excluded from the study. The demographic characteristics of the subjects, including hand dominance as determined using the Edinburgh Hand Preference Inventory, years of education and features of the disease in migraineurs such as age at onset of disease, disease duration, headache frequency, headache duration, and the presence of aura, were all recorded. The Beck Depression Inventory (BDI) and Beck Anxiety Inventory (BAI) were used to evaluate depression and anxiety symptoms in all participants of the study.

The presence and severity of RLS were assessed using 2012 Revised IRLSSG Diagnostic Criteria for RLS [24] and RLS rating scale [25], respectively. The diagnosis of RLS depended on the existence of these five criteria: an urge to move the legs (1) usually but not always with abnormal sensation in the legs, (2) with any accompanying unpleasant sensations beginning or worsening during periods of rest or inactivity, (3) with any accompanying unpleasant sensations, partially or totally relieving by movement, such as walking or stretching, at least as long as the activity continues, (4) during rest or inactivity only occurring or is worse in the evening or night than during the day, (5) the occurrence of these features is not solely accounted for as symptoms primary to another medical or a behavioral condition [24]. The RLS rating scale includes a total of ten questions; the scaling of RLS severity is as follows: mild severity, 0–10; moderate severity, 11–20; severe, 21–30; very severe, 31–40 [25]. Among migraineurs, only patients with a diagnosis of RLS for at least a year were included.

MRI acquisition parameters

MRI examinations were performed on a 1.5 Tesla Philips Achiva (Philips Medical Systems, Eindhoven, Netherlands) using an 8-channel sense head coil with the subjects in the supine position, lasting approximately 8–10 min for each subject. Survey images, T2-weighted transverse slices (TR, 4000 ms; TE, 90 ms; slice thickness, 5 mm), and 140 three-dimensional (3D) T1-weighted gradient-echo contiguous coronal slices (slice thickness, 1.2 mm; TE, 4.6 ms; TR, 30 ms; flip angle, 30°; field of view, 256 mm; voxel size, 1 × 1) were obtained.

Volumetric MRI measurements (manual, VBM, and volBrain measurements)

Manual measurements

The manual volumetric measurements of the bilateral caudate nucleus and putamen were performed by using the software program AFNI (Analysis of Functional Neuroimaging) developed by the National Institutes of Health. Although AFNI was developed as a functional MRI (fMRI) tool, it also has the feature of manual volumetric measurements, which enables the simultaneous tracing of brain structures on the three planes (i.e., sagittal, axial, and coronal). Tracings were made on T1-weighted MRIs following a particular protocol for each structure (Fig. 1). AFNI calculated the volume of the structure by multiplying the pixels by the voxel volume. Each structure was traced through the slices between the first slice and the last slice where it was seen based on the medial, lateral, superior, and inferior boundaries determined for the given structure.

Total intracranial volume

The superior edge of the foramen magnum was considered the inferior border. The cerebrospinal fluid (CSF) surrounding the brain parenchyma was not included in the tracings. The brain was measured in every other slice.

Caudate volume measurement

The coronal plane was used as the gold standard plane, although tracings were made on the three planes. Measurements started from the last slice chosen as the slice where the caudate was seen on the lateral part of the anterior horn of the lateral ventricle. The caudate was traced every other three slices until the slice where the nucleus accumbens was first seen. The internal capsule was the lateral and inferior boundary between caudate and putamen until the slice where the nucleus accumbens emerged. The anterior horn of the lateral ventricle was the medial boundary, and the white matter was the superior boundary in these slices (Fig. 1a). Starting from the slice where the nucleus accumbens was first seen, the

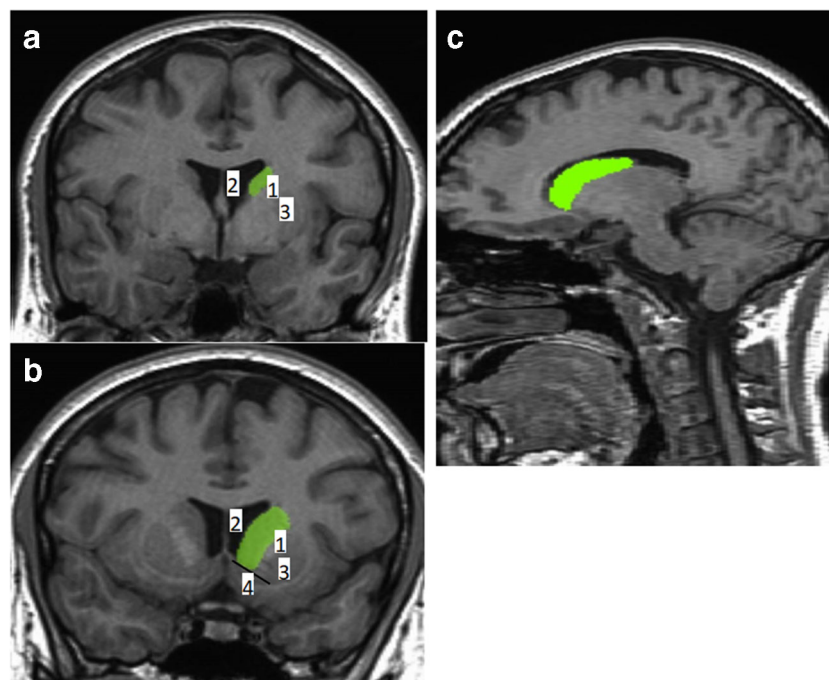


Fig. 1 Caudate tracings on T1-weighted MRI images via AFNI (green area shows caudate nucleus). **a** Caudate tracings in the posterior coronal slices: the manual delineation of the caudate started from the very most posterior slice where it was first seen. In these posterior slices, the internal capsule (1) was the lateral and inferior boundary, the anterior (frontal) horn of the lateral ventricle (2) was the medial boundary, and the surrounding white matter was set as the superior boundary. (3) Putamen. **b** Caudate tracings in the slices where the nucleus accumbens was seen: in

these slices, the inferior border (i.e., separation of the caudate from the nucleus accumbens) was determined by the line drawn from the most inferior point of the anterior horn of the lateral ventricle to the most inferomedial point of the internal capsule. The lower part of this line was considered nucleus accumbens and not included in the measurement. (1) Internal capsule, (2) anterior (frontal) horn of the lateral ventricle, (3) putamen, (4) nucleus accumbens. **c** Caudate tracings were completed in the sagittal plane

inferior border (i.e., separation of the caudate from the nucleus accumbens) was determined by the line drawn from the most inferior point of the anterior horn of the lateral ventricle to the most inferomedial point of the internal capsule. The lower part of this line was considered nucleus accumbens and not included in the measurement (Fig. 1b). Following the coronal tracings as a guide, the tracing was completed on the sagittal plane (Fig. 1c). The axial plane was used to review and adjust the tracings where necessary.

Putamen volume measurement

The tracings for the putamen volumetry started on the coronal plane. The first slice was the slice where the putamen was first seen as lateral and inferior to the caudate. The boundaries were as follows: medially internal capsule, laterally external capsule, superiorly, and inferiorly white matter (Fig. 2a). In the coronal slices where nucleus accumbens disappears and the globus pallidus is seen, sometimes, it becomes difficult to delineate the lateral border of the putamen. Therefore, we traced putamen every three–four slices where the lateral border was more distinct in the posterior slices. The separation of

putamen from the nucleus accumbens was made the way as it was made in the caudate volumetry protocol, by a line drawn between the most inferior point of the anterior horn of the lateral ventricle and the most inferomedial point of the internal capsule (Fig. 2b). The lateral border of the putamen is particularly more distinct on the axial plane. Therefore, following the guiding tracings made on the coronal plane, the putamen was traced every other three to four slices on the axial plane (Fig. 2c). Finally, using the tracings made on the coronal and axial planes as a guide, the tracing was completed on the sagittal plane (Fig. 2d). The tracings were checked on the axial and coronal planes for the lateral border (external capsule) and medial border (globus pallidus) before the finalization of the tracing process.

The TIVs were measured by four medical students (O.C., M.Ü., O.U.T., and E.S) whose inter-rater reliabilities were determined on 10 brains, and the intra-class correlation coefficients (ICCs) according to the measurements of K.Y. were all above 0.98, and the intra-rater reliability for each rater of the ICC was above 0.97. The caudate and putamen volumes were measured by K.Y. who was blinded to each subject's group. The intra-rater reliabilities using ICCs, determined in

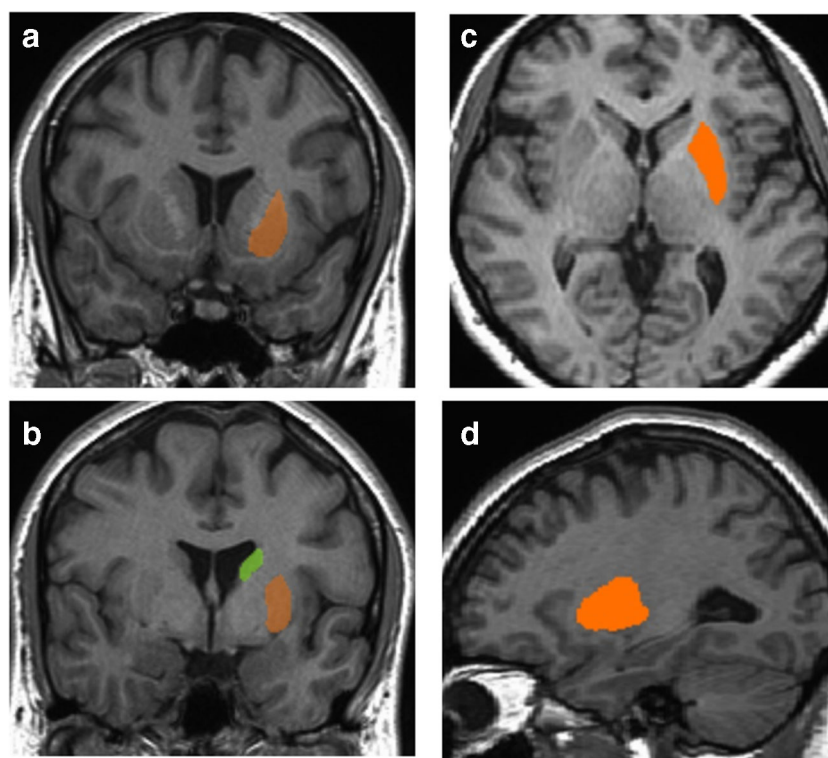


Fig. 2 Putamen tracings on T1-weighted MRI images via AFNI (green area shows caudate nucleus and orange area shows putamen). **a** Putamen tracings in the anterior coronal slices: the manual delineation of the putamen started from the very most anterior slice where it was first seen. In these anterior coronal slices, the internal capsule was the medial boundary; the external capsule was the lateral boundary. The superior and inferior boundaries were set as the surrounding white matter. **b** Putamen

tracings in the posterior coronal slices: the putamen and nucleus accumbens were separated by the same way with caudate. **c** Putamen tracings in the axial plane: the lateral boundary of putamen is particularly more distinct in the axial plane. The coronal tracings were corrected accordingly in the axial plane. **d** Putamen tracings in the sagittal plane: the tracings were completed in the sagittal plane as we did for the caudate tracings

ten brains, for the right caudate and left caudate, were 0.95 and 0.98, respectively. The ICCs for the right and left putamen were 0.95 and 0.89, respectively.

Voxel-based morphometry analysis

VBM is one of the morphometric methods. It became popular owing to its easiness of use and credible results. By using statistical parametric mapping, VBM enables the characterization of small-scale differences in brain anatomy. It is a simple and objective tool that makes a voxel-wise comparison of the local concentration of GM between two groups of subjects possible throughout the entire brain on MR images with high regional specificity [26–27].

This study used the CAT12 (Computational Anatomy Toolbox) which uses and extends the new unified segmentation approach implemented in Statistical Parametric Mapping (SPM12), executed in Matlab 7.10.0 (R2010a) for the whole-brain volumetric analysis. The sagittal T1 DICOM (Digital Imaging and Communications in Medicine) files were converted to NIFTI-1 (Neuroimaging Informatics Technology Initiative) format. The converted files were then segmented into gray and white matter and normalized using the unified model cited above. Three tissue components, namely the gray matter (GM), white matter (WM), and CSF, were obtained to calculate the overall tissue volume (GM, WM, and CSF volume) and TIV in the native space. The Automated Anatomical Labeling (AAL) atlas delivered as part of the SPM toolboxes was used for calculating the lobar GM volumes. This atlas does not map the nucleus accumbens.

To identify the brain morphological changes in the groups, we performed two whole-brain VBM analyses using the CAT12 toolbox. Whole-brain statistical analyses were performed in CAT12 using the spatially normalized and smoothed GM maps to assess whole-brain effects. Second-level general linear models were specified including the following two groups: control and migraine. First, a two-sample *t* test was performed to compare the GM volume between the two groups. For all analyses, we included TIV, age, BDI score, BAI score, and years of education as covariates. Finally, the normalized GM images were smoothed using a Gaussian filter (8 mm full-width half-maximum, FWHM). Statistical significance was defined at $p < 0.05$ after cluster-level family-wise error correction (cFWE).

volBrain analysis

Unlike many other automated or semi-automated volumetric packages such as FreeSurfer, VolBrain does not require any installation, configuration, and training [28]. It is free, user-friendly, works fast (in few minutes), and gives more

reproducible and accurate results compared with similar software packages such as FreeSurfer and FIRST [28–31] with lower segmentation failure rates [29].

The whole-brain volumetric analysis was also performed by uploading the anonymized compressed T1-weighted images in NIFTI format to the online “volBrain” MRI brain volumetry system. volBrain is a pipeline of processes aimed at automatically analyzing MRI brain data and producing PDF reports with the volumes of the total intracranial cavity tissues (CSF, GM, and WM) with the bilateral volumes of the following structures: caudate, putamen, globus pallidus, nucleus accumbens, thalamus, hippocampus, amygdala, cerebellum, brainstem, and label maps after an average processing time of 12 min.

Statistical analysis

The statistical analyses of the clinical data were performed using the IBM SPSS 22.0 program. Chi-square and Fisher’s exact test were used for the analysis of categorical data. One-way analysis of variance (ANOVA) was used to determine differences in group categories when the *p* value from the ANOVA test statistics is statistically significant, post hoc multiple comparisons (Tukey’s HSD) were used to know which group differ from which others. The statistical analyses of the neuroimaging data were performed as follows: the Shapiro-Wilk test was used, and histograms and q-q plots were formed to assess the normality of data distribution. The Levene test was used to test variance homogeneity. Volumes were analyzed by using one-way ANOVA, for the groups, RLS₁, RLS₀, and control groups. ANCOVA was performed to adjust for the effect of age, years of education, TIV, BDI scores, and BAI scores. Following significant group main effects, post hoc analyses were conducted using Tukey’s honestly significant difference (HSD) and the Bonferroni correction for ANOVAs and ANCOVAs, respectively. The degree of association between continuous variables, such as frequency per month and caudate and putamen volumes, was calculated by Pearson’s correlation coefficient and summarized by Pearson’s rho and related *p* values.

Results

There were 37 right-handed female patients in the study group and 17 healthy right-handed females in the control group. The mean ages of the patients and controls were 33.18 ± 1.23 (range, 19–44) years and 31.9 ± 1.6 (range, 20–45) years, respectively. The demographic data are presented in Table 1. The migraine group as a whole, RLS₀ and RLS₁ subgroups of patients, had fewer years of education than the control group ($p < 0.05$). The migraine group as a whole and RLS₁ group of patients had higher BDI scores than the control group ($p <$

Table 1 Demographic and clinical characteristics of the patient groups and the control group

Demographic and clinical data	Migraineurs (<i>n</i> = 37)	RLS ₁ (<i>n</i> = 18)	RLS ₀ (<i>n</i> = 19)	Control group (<i>n</i> = 17)	<i>p</i> value
Age, years (mean ± SD)	33.18 ± 1.23	34.5 ± 1.8	31.9 ± 1.6	31.9 ± 1.6	0.460 ^a
BDI score (mean ± SD)	19.18 ± 1.95	22.33 ± 2.77	15.84 ± 2.67	11.7 ± 2.42	0.024 ^{a*}
BAI score (mean ± SD)	17.16 ± 2.23	22.66 ± 3.32	11.94 ± 2.55	7.64 ± 1.82	0.001 ^{a*}
Years of education (mean ± SD)	8.97 ± 0.87	9.89 ± 1.23	8.00 ± 1.21	14.58 ± 1.47	0.003 ^{a*}
TIV, mm ³ (mean ± SD)	1278.49 ± 16.10	1234.57 ± 20.18	1320.10 ± 21.17	1329.10 ± 25.74	0.007 ^{a*}
Duration of migraine disease, months (mean ± SD)	106.45 ± 14.92	82.89 ± 14.01	131.33 ± 26.05		0.106 ^b
Frequency of migraine attack per month (mean ± SD)	10.21 ± 1.72	9.84 ± 2.31	10.61 ± 2.64		0.827 ^b
Duration of headache, hours (mean ± SD)	29.81 ± 4.32	29.57 ± 5.96	30.05 ± 6.46		0.957 ^b
Age at onset, years (mean ± SD)	24.29 ± 1.44	24.94 ± 1.91	23.61 ± 2.22		0.651 ^b
Presence of aura migraineurs					
With aura (<i>n</i>)	22 (100%)	13 (59.1%)	9 (40.9%)		0.124 ^c
Without aura (<i>n</i>)	15 (100%)	5 (33.3%)	10 (66.7%)		
Severity of RLS					
Mild (<i>n</i>)		2 (11.1%)			
Moderate (<i>n</i>)		9 (50%)			
Severe (<i>n</i>)		6 (33.3%)			
Very severe (<i>n</i>)		1 (5.5%)			

RLS₀, migraine patients without RLS; RLS₁, migraine patients with comorbid RLS; SD, standard deviation; BDI, Beck Depression Inventory; BAI, Beck Anxiety Inventory; TIV, total intracranial volume

^a One-way analysis of variance test

^b Independent samples *t* test

^c Chi-square test

**p* < 0.05

0.05). The RLS₁ group had higher BAI scores than the migraine group as a whole, RLS₀ group, and the control group (*p* < 0.05). The RLS₁ group had lower TIV values compared with migraine group as a whole, RLS₀, and control groups (*p* < 0.05). There were no differences in the ratios of patients with and without aura between the RLS₁ and RLS₀ groups (*p* > 0.05). No differences were found between the RLS₁ and RLS₀ groups in terms of the duration of migraine disease, frequency of attacks per month, duration of headache, and age at disease onset (*p* > 0.05). According to the RLS rating scale, most of the patients had moderate or severe RLS (*n* = 9, 50% and *n* = 6, 33.3%, respectively), whereas two patients showed mild (11.1%) and one patient showed very severe (5.5%) symptoms. The RLS₁ group patients had a mean RLS scale rating score of 19.39 ± 7.171.

Migraineurs with/without RLS vs controls

The results of the statistical analyses in the manual and volBrain measurements via variance analysis (one-way ANOVA) among the three groups (RLS₁, RLS₀, and control group) are shown in Table 2. Following the post hoc analyses, we found larger left caudate sizes in the RLS₀ group compared with the control group (*p* = 0.047). We found no other statistical differences after covarying for these variables among the three groups.

In our VBM analyses, the RLS₁ patients had larger left superior occipital gyrus and precuneus when compared with the RLS₀ patients. The GMVs of the substantia nigra (SN), mammillary bodies, and cuneus were decreased in the RLS₁ group when compared with the RLS₀ group (Fig. 3). Patients in the RLS₁ group had increased GMVs of the superior temporal gyrus (STG), Brodmann area 38, and left insula compared with the control group, whereas there were decreases in the volumes of the splenium of corpus callosum (CC) and bilateral cerebrum sub-lobar white matter regions in this patient group compared with the controls (Fig. 3). The RLS₀ group had increased volumes of the Brodmann area 22, right STG, and Heschl gyrus compared with the controls. The volumes of the frontal sub-gyral white matter and genu of CC were decreased in the RLS₀ group compared with the control group (Fig. 3).

Migraineurs vs controls

The total caudate, right caudate, and left caudate volumes were larger in migraineurs than in the controls (adjusted *p* = 0.019, *p* = 0.009, and *p* = 0.008, respectively) in volBrain measurements. The right caudate volume was also larger in migraineurs compared with controls when measured manually (adjusted *p* = 0.016). There were positive and moderate relations between

Table 2 Comparison of volumes among RLS₁, RLS₀, and control groups

Volumes (mm ³)	Groups			<i>p</i> ^a	Pairwise comparisons <i>p</i> ^b			Adjusted <i>p</i> ^c
	Control (<i>n</i> = 17) Mean ± SD	RLS ₀ (<i>n</i> = 19) Mean ± SD	RLS ₁ (<i>n</i> = 18) Mean ± SD		RLS ₁ vs. RLS ₀	RLS ₁ vs. Control	RLS ₀ vs. Control	
Manual measurements								
R caudate	3732.39 ± 402.29	4049.61 ± 578.49	3787.00 ± 542.16	0.149	(1.000)	(0.055)	(0.072)	0.031*
L caudate	3919.13 ± 493.17	4071.14 ± 473.03	3809.35 ± 608.45	0.325				0.579
R putamen	4469.41 ± 375.95	4747.16 ± 525.44	4587.91 ± 565.98	0.253				0.227
L putamen	4406.51 ± 377.30	4602.04 ± 474.90	4561.50 ± 654.52	0.500				0.271
volBrain measurements								
Total WM	524.09 ± 77.36 ^a	517.66 ± 54.470 ^a	466.95 ± 48.21 ^b	0.013*	0.038 ^x	0.021 ^x	0.946	0.861
Total GM	656.02 ± 54.63	661.34 ± 63.28	617.62 ± 60.93	0.066				0.852
Intracranial cavity	1329.11 ± 106.13 ^a	1320.11 ± 92.29 ^a	1234.58 ± 85.64 ^b	0.007*	0.022 ^x	0.013 ^x	0.956	0.997
Total cerebrum GM	558.55 ± 48.25	563.83 ± 56.01	524.44 ± 52.88	0.059				0.786
Total cerebrum WM	468.19 ± 67.55 ^a	465.09 ± 47.67 ^a	419.08 ± 43.33 ^b	0.013*	0.031 ^x	0.024 ^x	0.984	0.926
Total R cerebrum GM	279.57 ± 24.39 ^{ab}	282.09 ± 27.87 ^a	261.85 ± 26.38 ^b	0.050*	0.060	0.125	0.956	0.772
Total R cerebrum WM	235.94 ± 34.24 ^a	233.35 ± 23.74 ^a	210.18 ± 21.93 ^b	0.011*	0.031 ^x	0.018 ^x	0.955	0.863
Total L cerebrum GM	278.97 ± 23.98	281.74 ± 28.24	262.59 ± 26.54	0.071				0.797
Total L cerebrum WM	232.25 ± 33.38 ^a	231.73 ± 23.98 ^a	208.90 ± 21.48 ^b	0.016*	0.031 ^x	0.032 ^x	0.998	0.967
Total cerebellum	130.94 ± 9.88 ^a	128.40 ± 7.18 ^a	120.59 ± 10.94 ^b	0.005*	0.039 ^x	0.006 ^x	0.700	0.359
R cerebellum	65.63 ± 4.89 ^a	64.35 ± 4.02 ^a	60.35 ± 5.48 ^b	0.005*	0.039 ^x	0.006 ^x	0.709	0.311
L cerebellum	65.31 ± 5.09 ^a	64.05 ± 3.40 ^a	60.23 ± 5.62 ^b	0.007*	0.048 ^x	0.008 ^x	0.709	0.449
Total cerebellum GM	91.60 ± 9.67	91.81 ± 7.84	87.63 ± 10.16	0.318				0.966
Total cerebellum WM	42.87 ± 17.78 ^a	36.59 ± 7.20 ^{ab}	32.95 ± 6.07 ^b	0.042*	0.599	0.034 ^x	0.234	0.064
R cerebellum GM	44.81 ± 4.94	45.02 ± 4.00	43.11 ± 5.36	0.425				0.988
R cerebellum WM	20.82 ± 5.49 ^a	19.33 ± 3.87 ^{ab}	17.24 ± 3.03 ^b	0.050*	0.297	0.040 ^x	0.547	0.433
L cerebellum GM	46.79 ± 4.84	46.79 ± 4.01	44.52 ± 4.92	0.241				0.925
L cerebellum WM	18.52 ± 5.18	17.26 ± 3.40	15.71 ± 3.13	0.120				0.720
Brainstem	22.49 ± 2.47 ^a	21.74 ± 2.04 ^{ab}	20.51 ± 1.62 ^b	0.022*	0.177	0.018 ^x	0.525	0.163
Total caudate	6.43 ± 0.54	6.78 ± 0.72	6.39 ± 0.86	0.204				0.060
R caudate	3.24 ± 0.26	3.43 ± 0.36	3.23 ± 0.44	0.191	(1.000)	(0.083)	(0.111)	0.049*
L caudate	3.02 ± 0.81	3.36 ± 0.36	3.16 ± 0.42	0.205	(1.000)	(0.073)	(0.047 ^y)	0.028*
Total putamen	7.72 ± 0.77	7.95 ± 0.76	7.63 ± 0.89	0.473				0.235
R putamen	3.84 ± 0.36	3.96 ± 0.35	3.80 ± 0.43	0.409				0.378
L putamen	3.88 ± 0.42	3.99 ± 0.42	3.83 ± 0.46	0.545				0.158
Thalamus	10.82 ± 1.09	10.79 ± 1.01	10.18 ± 1.04	0.126				0.960
R thalamus	5.35 ± 0.53	5.36 ± 0.53	5.09 ± 0.50	0.212				0.776
L thalamus	5.47 ± 0.62	5.43 ± 0.50	5.09 ± 0.58	0.101				0.981
Total globus pallidus	1.76 ± 0.20	1.84 ± 0.33	1.86 ± 0.27	0.568				0.273
R globus pallidus	0.89 ± 0.10	0.89 ± 0.19	0.91 ± 0.13	0.869				0.562
L globus pallidus	0.87 ± 0.13	0.95 ± 0.16	0.94 ± 0.15	0.242				0.124
Hippocampus	7.50 ± 0.62	7.59 ± 0.54	7.39 ± 0.68	0.620				0.625
R hippocampus	3.81 ± 0.33	3.82 ± 0.31	3.71 ± 0.35	0.557				0.805
L hippocampus	3.69 ± 0.32	3.76 ± 0.29	3.68 ± 0.35	0.671				0.556
Amygdala	1.22 ± 0.13	1.22 ± 0.23	1.23 ± 0.23	0.987				0.271
R amygdala	0.62 ± 0.07	0.62 ± 0.14	0.61 ± 0.14	0.967				0.604
L amygdala	0.60 ± 0.07	0.60 ± 0.10	0.62 ± 0.10	0.826				0.100
Nucleus accumbens	0.58 ± 0.09	0.61 ± 0.11	0.56 ± 0.09	0.227				0.624
R nucleus accumbens	0.27 ± 0.04	0.28 ± 0.04	0.26 ± 0.05	0.189				0.772
L nucleus accumbens	0.31 ± 0.05	0.32 ± 0.07	0.30 ± 0.05	0.388				0.605

RLS₀, migraine patients without RLS; RLS₁, migraine patients with comorbid RLS; SD, standard deviation; R, right; L, left; WM, white matter; GM, gray matter

^a *p* value of one-way analysis of variance (ANOVA) test

^b *p* value of Tukey’s HSD test and the Bonferroni correction

^c *p* value of one-way analysis of covariance (ANCOVA) test

^x Significant values for Tukey’s HSD (values outside of parentheses are *p* values)

^y Significant values for the Bonferroni correction (values in parentheses are normalized *p* values)

**p* < 0.05

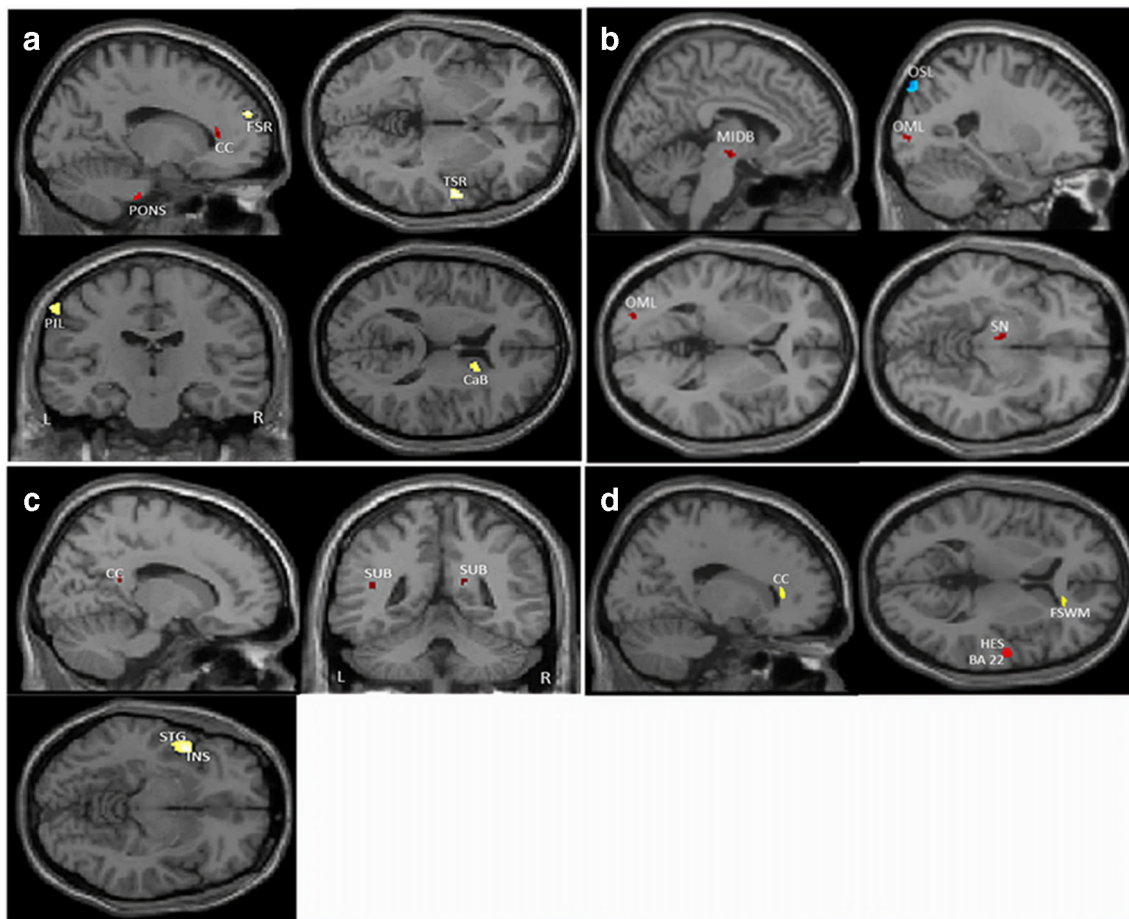


Fig. 3 Brain morphological changes in migraine patients, RLS₁, RLS₀, and control groups in single T1-weighted MRI images ($p < 0.001$, uncorrected) via VBM. **a** Altered structural volumes in migraine and control groups. Yellow area shows volume increase; red area shows volume decrease in the migraine group. FSR, frontal superior right; TSR, temporal superior right; CC, corpus callosum; PIL, parietal inferior left; CaB, caudate body. **b** Altered structural volumes in RLS₁ and RLS₀ groups. Blue area shows volume increase; red area shows volume decrease in the RLS₁ group. MIDB, midbrain; OSL, occipital

superior left; OML, occipital middle left; SN, substantia nigra. **c** Altered structural volumes in RLS₁ and control groups. Yellow area shows volume increase; red area shows volume decrease in the RLS₁ group. SUB, sub-lobar; STG, superior temporal gyrus; INS, insula. **d** Altered structural volumes in RLS₀ and control groups. Red area shows volume increase; yellow area shows volume decrease in the RLS₀ group. FSWM, frontal sub-gyral white matter; HES, Heschl gyrus; BA 22, Brodmann area 22. L, left; R, right

attack frequency per month and caudate and putamen volumes (right caudate measured manually: $r = 0.579$, $p < 0.001$; left caudate measured manually: $r = 0.476$, $p = 0.003$; right putamen measured manually: $r = 0.397$, $p = 0.015$; left putamen measured manually: $r = 0.389$, $p = 0.017$; total caudate via VolBrain: $r = 0.391$, $p = 0.017$; right caudate via volBrain: $r = 0.400$, $p = 0.014$; and left caudate via volBrain: $r = 0.380$, $p = 0.020$; data not shown). The total cerebellum WM was smaller in migraineurs relative to the control group in volBrain measurements (adjusted $p = 0.020$).

Based on the VBM analyses, in comparison with controls, migraineurs had increased GMVs in the right STG, right superior frontal gyrus, Brodmann area 10, body of the caudate, and left inferior parietal gyrus. On the other hand, migraineurs

showed GMV reductions in the pons and genu of CC when compared with the control group (Fig. 3).

Discussion

The primary goal of our study was to compare the volumes of brain structures between migraine patients with and without RLS by using three measurement techniques: manual measurements, volBrain, and VBM. The manual measurements did not result in any volumetric differences in caudate and putamen volumes between the RLS₀ and RLS₁ groups. volBrain analyses revealed that the RLS₀ group had increased left caudate volumes compared with controls. Based on the VBM analyses, we found increased

left superior occipital gyrus and precuneus volumes and decreased volumes of SN, mammillary bodies, and cuneus in the RLS₁ group compared with the RLS₀ group. The RLS₁ group had more GMV in the STG, Brodmann area 38, and left insula, and less GMV in the splenium of CC and cerebral sub-lobar WM regions compared with the control group. On the other hand, the RLS₀ group had larger volumes of Brodmann area 22, right STG, and Heschl gyrus, and smaller volumes of the genu of CC and frontal sub-gyral WM compared with the control group.

Overall, the migraineurs had larger total caudate volumes based on the volBrain measurements and right caudate volume based on the manual measurements. Altogether, the migraineurs had increased GMVs of the right STG, right superior frontal gyrus, Brodmann area 10, body of the caudate, and left inferior parietal gyrus compared with the control group, whereas there were decreases in the volumes of the pons and CC (anteriorly) in this patient group compared with the controls.

Volumetric findings between RLS₁ group and RLS₀ group

Volumetric changes in several brain structures have been referred to different features of migraine, e.g., treatment response [32], frequency of migraine attacks [33, 34], disease duration [35], and genetic profile [36]. Disorders accompanying migraine might act as confounding factors for the volumetric findings reported in this population. For instance, migraineurs with depression had smaller GM and WM volumes compared with those without depression [37]. The functional connectivity between the hippocampus and medial prefrontal cortex was found to correlate negatively with anxiety scores in migraine patients [36]. RLS, on the other hand, is the focus of our attention because both migraine and RLS share common pathophysiologic pathways throughout the dopaminergic system [16]. The risk of developing RLS among migraine patients is high (up to five times) in relation to dopaminergic symptoms (e.g., yawning, nausea, food cravings) [38].

Until today, volumetric changes in migraine patients with RLS have been investigated only in one VBM study by Yang et al. [17]. The design of their study differed from ours because they also included patients with RLS in addition to migraineurs with and without RLS and a control group. The authors reported an increased volume of the right middle frontal gyrus in migraine patients with comorbid RLS. The analyses of brain volumes in our study via three different techniques resulted in a wider spectrum of volumetric changes among migraine patients with and without RLS and controls.

We found a decrease in SN size only in migraineurs with RLS. The SN is the source of the nigrostriatal dopaminergic pathway. A popular theory on the pathophysiology of RLS is that the dopamine-containing neurons in the SN, which project to the striatum, have low iron levels [11] resulting in the disruption of dopaminergic function by limiting either tyrosine hydroxylase activity or the expression of dopamine transporters and receptors. The SN has been reported to have decreased iron stores in migraine patients, which may contribute to an increase in the risk of developing RLS [39]. It seems that SN pathology accompanies migraine under the existence of comorbidity of RLS.

Both the RLS₁ and RLS₀ groups had decreased CC volumes compared with the controls. This defect, however, differed topographically between these two patient groups. With the comorbidity of RLS, the deficit in the CC shifted more dorsally to the splenium region, whereas all migraineurs and the RLS₀ group had decreases in CC volumes anteriorly, i.e., in the genu of the CC. Consistent with our findings, diffusion tensor imaging (DTI) studies showed reduced white matter integrity in the genu of the CC in patients with migraine [40–41]. Deficits in the splenium and the body of the CC in addition to the genu have also been reported [40]. Genu has the highest density of myelinated axons and connects the prefrontal cortex and higher-order sensory areas [42]. The prefrontal cortex, with its connections with the basal ganglia, periaqueductal GM, and thalamus, is important in pain processing. Depending on the dopamine activation, it can induce pain chronification through frontostriatal pathways [43], emphasizing the critical role of this part of CC in the pathophysiology of pain disorders.

The posterior deficit in the CC might be related to the comorbidity of RLS according to our results. Rizzo et al. [17] reported a positive correlation with RLS rating scale scores and axial and mean diffusivity values in the splenium which might mean more space between axons in relation to disease severity. Chang et al. [44] reported decreased WM integrity in the genu of CC, rather than the splenium in patients with RLS. The splenium regulates thalamocortical inputs to the visual cortex [45]. The splenium has two groups of fibers. The thick fibers on the posterior part are derived from primary and secondary visual areas, and its anterior part contains fibers originating from the parietal and medial temporal association areas [46]. We also found increased left superior occipital gyrus volume and decreased cuneus volume in RLS₁ patients compared with RLS₀ patients. The superior occipital gyrus and cuneus are important structures in visual processing. Decreased functional connectivity in the sensorimotor and visual processing networks has been described in patients with RLS, which was attributed to dopaminergic hypoactivity and cortical deafferentation of the basal ganglia [47–48]. Visual information processing in the occipital lobes plays a critical role in the sensorimotor network because motor

responses are highly associated with visual stimuli. The results of our study indicate pathology in the visual processing network specific to migraineurs with RLS.

Yang et al. [18] reported decreased functional connectivity in both the visual and auditory networks, regardless of the comorbidity of RLS. Our volumetric findings differed from their functional neuroimaging findings. We found volumetric changes in structures related to visual processing only in the migraine patient group with accompanying RLS. On the other hand, we found volumetric increases in structures related to auditory processing (i.e., Brodmann area 22 and the Heschl gyrus) only in the RLS₀ group. It is hard to come to a conclusion as to whether increases in GM density reflect an increase in neurons or glial cells, synapses, and capillaries leading to overfunction or malfunction [49]. Migraine patients are reported to have deficits with central auditory processing with sound hypersensitivity between migraine attacks [50].

In our study, there was an increase in left insula volume in the RLS₁ group compared with the control group. Increased functional plasticity has been demonstrated in the insula bilaterally in patients with RLS [51]. Another fMRI study also showed higher functional activity in the insula in patients with RLS [48].

Volumetric findings between migraine patients and controls

The STG seems to be affected regardless of whether RLS accompanies migraine because we found increases in STG volumes in migraineurs, both RLS₁ and RLS₀ patients compared with controls. We have two explanations for this finding. The STG is actually a neglected area regarding its role in pain. Accordingly, there are few studies on STG pathology in the migraine literature. In a VBM study, volume reduction, rather than an increase in the right STG as we found in our study, was observed in patients with migraine compared with controls [52]. Decreased STG activation following induction of pain by a heat stimulus in patients with migraine was observed in an fMRI study [53]. STG is a multimodal structure with heterogeneity in its functions. It is involved in pain processing by monitoring mismatches between pain expectation and pain perception [54], pain anticipation [55], and execution of pain expression [56]. Based on the significant role of the STG in pain processing and STG deficits observed in functional and structural neuroimaging studies in a list of conditions related to pain such as fibromyalgia [57], somatoform pain disorder [58], and chronic idiopathic neck pain [54], we think that our finding might not be related to migraine pathophysiology but rather related to deficits in pain processing itself. Another possibility is that the response to treatment might affect STG size in patients with migraine. Hubbard et al. [19] found the increased cortical thickness of the STG in migraineurs who responded to treatment compared with

non-responders. However, their study had a total of only 24 patients and lacked a control group. We do not have information on treatment response in our patient sample; therefore, we could not take into consideration the effect of this parameter when analyzing the data.

After comparing the volumetric data of the migraine group as a whole with that of the control group, we found larger caudate volumes in the migraine group via the three modalities used in our study. The more migraine attacks meant a larger caudate, which is consistent with the findings of Maleki et al. [34]. Yuan et al. [35], however, found no relation between attack frequency and caudate volumes. On the other hand, the authors demonstrated a relation between increased monthly frequency of migraine attack and increased functional connectivity between the bilateral caudate and left insula. We also found a moderate positive relation between putamen volumes and attack frequency. Neeb et al. [33] reported increased putamen volumes in patients with episodic migraine and a positive correlation between putamen volumes and attack frequency in patients with episodic and chronic migraine. Rocca et al. [59] also reported larger putamen volumes in migraine patients compared with the controls in a pediatric population showing early involvement of putamen in the disorder.

Magon et al. [60] found decreased striatal volume (caudate + putamen) in patients with migraine. The mean monthly attack frequency was three times more in our sample than in the study of Magon et al. (10.2 vs. 3.2) [60]. Provided that more attacks result in larger caudate and putamen, both structures might increase in size as the number of attacks increase. Basal ganglia structures are considered to play different roles in pain processing, i.e., sensory, emotional/cognitive, and modulatory [38]. As proposed by Neeb et al. [33], increases in the sizes of these two structures might be the result of plasticity as an adaptive response to repetitive migraine attacks.

Although our study is not a technical report and it is beyond the scope of this article to compare the accuracy of different volumetric modalities, it might be worth discussing the different results gathered by the three different modalities in our study. We found caudate volumes larger only on the right side by the manual segmentation, and on both sides and total volumes as larger via volBrain in migraine patients compared with the controls. VBM analyses revealed a larger body of caudate in the patient group compared with the controls. The finding of larger left caudate in the RLS₀ group compared with the control group was a finding revealed by the volBrain analyses. We found correlations between attack frequency and caudate volumes based on both manual segmentation and volBrain methods but between attack frequency and putamen volumes obtained with manual segmentation only.

So far, the manual segmentation method has been considered the gold standard when comparing different neuroimaging quantitative modalities [28–30, 61]. VBM has been the most popular automated tool in structural MRI literature. It

gives us information on the GM density of all the structures in the brain. It is logical not to expect more than what volBrain offers in terms of volumetry of the brain structures as it only gives a restricted amount of brain structures, for the time being, a list of which was given in the “Methods” section. Ciampi et al. [62] found volumetric loss in the thalamus, hippocampus, and cerebellum in patients receiving natalizumab via FreeSurfer, a semi-automated volumetric software package, and these findings were not replicated in the VBM analyses. Lu et al. [63] found different findings on thalamus volumes with manual segmentation and FreeSurfer when comparing cirrhotic patients with the control group and inconsistent results on thalamus volume between FreeSurfer and VBM analyses. They explained this issue by referring to the existence of a mixture of white matter and gray matter in some voxels of the thalamus. It might be possible that volBrain, just like FreeSurfer does, might bring detailed information on the volumetric changes of the subcortical structures to the table than VBM does. The reasons beyond this exceed the aim of this study and require further investigation in the future.

A limitation of our study is its cross-sectional design. Another limitation is the small sample size, particularly in the migraine subgroups of patients with or without RLS. Unlike the study of Yang et al. [17], we had no isolated RLS patient group, which would have given us a deeper perspective. Another limitation, as mentioned before, is the medication status. We are unaware of either the response to the treatment status of our patient sample or the effects of these medications in the brain including medication overuse. Coppola et al. [64] reported a positive relation between the sizes of cerebellar hemispheres and the number of tablets taken per month. Additionally, medication overuse has been related to changes in brain structures [40]. As another limitation, we did not collect data on the duration of RLS in our study.

In conclusion, care should be given to the existence of comorbidity of RLS when planning quantitative neuroimaging studies with migraine patients. The deficits in the visual network in migraine seem to be related to the accompanying RLS, and deficits in the auditory network are particularly related to migraine pathology. STG is one of the important structures in pain-related disorders. More studies are required to further explore the relation of CC and its sub-regions in the pathophysiology of migraine and RLS because this structure's data are sparse in both disorders. Finally, we have replicated the relation between attack frequency and an increase in caudate and putamen volumes in migraine. The effective treatment of migraine is highly critical for the prevention of structural changes in the brains of migraine patients.

Acknowledgments We thank Ceyhan Türkmen for performing the statistical analysis of the data and David Chapman for editing the manuscript. We thank Dr. Ozan Cengiz, Dr. Meriç Ülgen, Dr. Orhun Ufuk Tipi, and Dr. Emir Şenocak for working as raters in TIV measurements.

Data availability The data used to support the findings of this study are available from the corresponding author upon reasonable request.

Funding information The authors received no specific funding for this work.

Compliance with ethical standards

Conflict of interest The authors declare that they have no conflict of interest.

Ethical approval All procedures performed in studies involving human participants were in accordance with the ethical standards of the institutional and/or national research committee and with the 1964 Helsinki Declaration and its later amendments or comparable ethical standards. The study was approved by the Ethics Committee of Dışkapı Yıldırım Beyazıt Training and Research Hospital, University of Health Sciences.

Informed consent Informed consent was obtained from all individual participants included in the study.

Consent for publication Patients signed informed consent regarding publishing their data.

References

- Burstein R, Noseda R, Borsook D (2015) Migraine: multiple processes, complex pathophysiology. *J Neurosci* 35:6619–6629. <https://doi.org/10.1523/JNEUROSCI.0373-15.2015>
- Yeh WZ, Blizzard L, Taylor BV (2018) What is the actual prevalence of migraine? *Brain Behav* 8(6):e00950. <https://doi.org/10.1002/brb3.950>
- Straube A, Andreou A (2019) Primary headaches during lifespan. *J Headache Pain* 20:35. <https://doi.org/10.1186/s10194-019-0985-0>
- Vos T, Abajobir AA, Abate KH et al (2016) Global, regional, and national incidence, prevalence, and years lived with disability for 328 diseases and injuries for 195 countries, 1990–2016: a systematic analysis for the Global Burden of Disease Study 2016. *Lancet* 390:1211–1259. [https://doi.org/10.1016/S0140-6736\(17\)32154-2](https://doi.org/10.1016/S0140-6736(17)32154-2)
- Linde M, Gustavsson A, Stovner LJ et al (2012) The cost of headache disorders in Europe: the Eurolight project. *Eur J Neurol* 19: 703–711. <https://doi.org/10.1111/j.1468-1331.2011.03612.x>
- Acar BA, Acar T, Alagöz AN et al (2016) Relationship between primary restless legs syndrome and migraine with aura. *Kaohsiung J Med Sci* 32:420–426. <https://doi.org/10.1016/j.kjms.2016.06.003>
- Becker PM (2015) Diagnosis of Restless Leg Syndrome (Willis-Ekbom Disease). *Sleep Med Clin* 10:235–240. <https://doi.org/10.1016/j.jsmc.2015.05.001>
- Koo BB (2015) Restless leg syndrome across the globe: epidemiology of the restless legs syndrome/Willis-Ekbom disease. *Sleep Med Clin* 10:189–205. <https://doi.org/10.1016/j.jsmc.2015.05.004>
- Schürks M, Winter A, Berger K et al (2014) Migraine and restless legs syndrome: a systematic review. *Cephalalgia* 34:777–794. <https://doi.org/10.1177/0333102414537725>
- Suzuki K, Suzuki S, Haruyama Y et al (2019) Restless legs syndrome is associated with headache-related disabilities in patients with migraine: a prospective 7-year follow-up study. *Eur J Neurol* 26:238–245. <https://doi.org/10.1111/ene.13796>
- Connor JR, Boyer PJ, Menzies SL et al (2003) Neuropathological examination suggests impaired brain iron acquisition in restless legs syndrome. *Neurology* 61:304–309. <https://doi.org/10.1212/wnl.0000078887.16593.12>

12. Hu W, Guo J, Chen N et al (2015) A meta-analysis of voxel-based morphometric studies on migraine. *Int J Clin Exp Med* 8:4311–4319.
13. Dai Z, Zhong J, Xiao P et al (2015) Gray matter correlates of migraine and gender effect: A meta-analysis of voxel-based morphometry studies. *Neuroscience* 299:88–96. <https://doi.org/10.1016/j.neuroscience.2015.04.066>
14. Jia Z, Yu S (2017) Gray matter alterations in migraine: a systematic review and meta-analysis. *Neuroimage Clin* 19:130–140. <https://doi.org/10.1016/j.nicl.2017.01.019>
15. Comley RA, Cervenka S, Palhagen SE et al (2012) A comparison of gray matter density in restless legs syndrome patients and matched controls using voxel-based morphometry. *J Neuroimaging* 22:28–32. <https://doi.org/10.1111/j.1552-6569.2010.00536.x>
16. Margariti PN, Astrakas LG, Tsouli SG et al (2012) Investigation of unmedicated early onset restless legs syndrome by voxel-based morphometry, T2 relaxometry, and functional MR imaging during the night-time hours. *AJNR Am J Neuroradiol* 33:667–672. <https://doi.org/10.3174/ajnr.A2829>
17. Rizzo G, Manners D, Vetrugno R et al (2012) Combined brain voxel-based morphometry and diffusion tensor imaging study in idiopathic restless legs syndrome patients. *Eur J Neurol* 19:1045–1049. <https://doi.org/10.1111/j.1468-1331.2011.03604.x>
18. Celle S, Roche F, Peyron R et al (2010) Lack of specific gray matter alterations in restless legs syndrome in elderly subjects. *J Neurol* 257:344–348. <https://doi.org/10.1007/s00415-009-5320-2>
19. Rizzo G, Li X, Galantucci S et al (2017) Brain imaging and networks in restless legs syndrome. *Sleep Med* 31:39–48. <https://doi.org/10.1016/j.sleep.2016.07.018>
20. Kurt S (2019) The comorbidity of migraine and restless legs syndrome. *Curr Neurol Neurosci Rep* 19:60. <https://doi.org/10.1007/s11910-019-0977-0>
21. Yang FC, Chou KH, Lee PL et al (2018) Patterns of gray matter alterations in migraine and restless legs syndrome. *Ann Clin Transl Neurol* 6:57–67. <https://doi.org/10.1002/acn3.680>
22. Yang FC, Chou KH, Hsu AL et al (2018) Altered brain functional connectome in migraine with and without restless legs syndrome: a resting-state functional MRI study. *Front Neurol* 9:25. <https://doi.org/10.3389/fneur.2018.00025>
23. Headache Classification Committee of the International Headache Society (2013) The International Classification of Headache Disorders, 3rd edition (beta version). *Cephalalgia* 33(9):629–808. <https://doi.org/10.1177/0333102413485658>
24. International Restless Legs Syndrome Study Group (IRLSSG) (2012) 2012 Revised IRLSSG Diagnostic Criteria for RLS. <http://irlssg.org/diagnosticcriteria>. Accessed: 28 February 2020
25. Walters AS, LeBrocq C, Dhar A et al; International Restless Legs Syndrome Study Group (2003) Validation of the International Restless Legs Syndrome Study Group rating scale for restless legs syndrome. *Sleep Med* 4(2):121–132. [https://doi.org/10.1016/s1389-9457\(02\)00258-7](https://doi.org/10.1016/s1389-9457(02)00258-7)
26. Whitwell JL (2009) Voxel-based morphometry: an automated technique for assessing structural changes in the brain. *J Neurosci* 29:9661–9664. <https://doi.org/10.1523/JNEUROSCI.2160-09.2009>
27. Ashburner J, Friston KJ (2001) Why voxel-based morphometry should be used. *Neuroimage* 14:1238–1243. <https://doi.org/10.1523/JNEUROSCI.2160-09.2009>
28. Manjón JV, Coupé P (2016) volBrain: an online MRI brain volumetry system. *Front Neuroinform* 10:30. <https://doi.org/10.3389/fninf.2016.00030>
29. Akudjedu TN, Nabulsi L, Makelyte M et al (2018) A comparative study of segmentation techniques for the quantification of brain subcortical volume. *Brain Imaging Behav*. 12:1678–1695. <https://doi.org/10.1007/s11682-018-9835-y>
30. Hannoun S, Tutunji R, El Homsy M et al (2019) Automatic thalamus segmentation on unenhanced 3D T1 weighted images: comparison of publicly available segmentation methods in a pediatric population. *Neuroinformatics* 17:443–450. <https://doi.org/10.1007/s12021-018-9408-7>
31. Naess-Schmidt E, Tietze A, Blicher JU et al (2016) Automatic thalamus and hippocampus segmentation from MP2RAGE: comparison of publicly available methods and implications for DTI quantification. *International Journal of Computer Assisted Radiology and Surgery*. 11:1979–1991. <https://doi.org/10.1007/s11548-016-1433-0>
32. Hubbard CS, Becerra L, Smith JH et al (2016) Brain changes in responders vs. non-responders in chronic migraine: markers of disease reversal. *Front Hum Neurosci* 10:497. <https://doi.org/10.3389/fnhum.2016.00497>
33. Neeb L, Bastian K, Villringer K et al (2017) Structural gray matter alterations in chronic migraine: implications for a progressive disease? *Headache* 57:400–416. <https://doi.org/10.1111/head.13012>
34. Maleki N, Becerra L, Nutile L et al (2011) Migraine attacks the basal ganglia. *Mol Pain* 7:71. <https://doi.org/10.1186/1744-8069-7-71>
35. Yuan K, Zhao L, Cheng P et al (2013) Altered structure and resting-state functional connectivity of the basal ganglia in migraine patients without aura. *J Pain* 14:836–844. <https://doi.org/10.1016/j.jpain.2013.02.010>
36. Liu J, Lan L, Mu J et al (2015) Genetic contribution of catechol-O-methyltransferase in hippocampal structural and functional changes of female migraine sufferers. *Hum Brain Mapp* 36:1782–1795. <https://doi.org/10.1002/hbm.22737>
37. Gudmundsson LS, Scher AI, Sigurdsson S et al (2013) Migraine, depression, and brain volume: the AGES-Reykjavik Study. *Neurology* 80:2138–2144. <https://doi.org/10.1212/WNL.0b013e318295d69e>
38. Cologno D, Cicarelli G, Petretta V et al (2008) High prevalence of dopaminergic premonitory symptoms in migraine patients with restless legs syndrome: a pathogenetic link? *Neurol Sci* 29:166–168. <https://doi.org/10.1007/s10072-008-0915-4>
39. Welch KM, Nagesh V, Aurora SK et al (2001) Periaqueductal gray matter dysfunction in migraine: cause or the burden of illness? *Headache* 41:629–637. <https://doi.org/10.1046/j.1526-4610.2001.041007629.x>
40. Shibata Y, Ishiyama S, Matsushita A (2018) White matter diffusion abnormalities in migraine and medication overuse headache: A 1.5-T tract-based spatial statistics study. *Clin Neurol Neurosurg* 174:167–173. <https://doi.org/10.1016/j.clineuro.2018.09.022>
41. Yu D, Yuan K, Qin W et al (2013) Axonal loss of white matter in migraine without aura: a tract-based spatial statistics study. *Cephalalgia* 33:34–42. <https://doi.org/10.1177/0333102412466964>
42. van der Knaap LJ, van der Ham IJ (2011) How does the corpus callosum mediate interhemispheric transfer? A review. *Behav Brain Res* 223:211–221. <https://doi.org/10.1016/j.bbr.2011.04.018>
43. Ong WY, Stohler CS, Herr DR (2019) Role of the prefrontal cortex in pain processing. *Mol Neurobiol* 56:1137–1166. <https://doi.org/10.1007/s12035-018-1130-9>
44. Chang Y, Paik JS, Lee HJ et al (2014) Altered white matter integrity in primary restless legs syndrome patients: diffusion tensor imaging study. *Neurol Res* 36:769–774. <https://doi.org/10.1179/1743132814Y.0000000336>
45. Williams MR, Sharma P, Macdonald C et al (2019) Axonal myelin decrease in the splenium in major depressive disorder. *Eur Arch Psychiatry Clin Neurosci* 269:387–395. <https://doi.org/10.1007/s00406-018-0904-4>
46. Knyazeva MG (2013) Splenium of corpus callosum: patterns of interhemispheric interaction in children and adults. *Neural Plast* 2013:639430. <https://doi.org/10.1155/2013/639430>

47. Liu C, Wang J, Hou Y et al (2018) Mapping the changed hubs and corresponding functional connectivity in idiopathic restless legs syndrome. *Sleep Med* 45:132–139. <https://doi.org/10.1016/j.sleep.2017.12.016>
48. Liu C, Dai Z, Zhang R et al (2015) Mapping intrinsic functional brain changes and repetitive transcranial magnetic stimulation neuromodulation in idiopathic restless legs syndrome: a resting-state functional magnetic resonance imaging study. *Sleep Med* 16:785–791. <https://doi.org/10.1016/j.sleep.2014.12.029>
49. Duerden EG, Laverdure-Dupont D (2008) Practice makes cortex. *J Neurosci* 28:8655–8657. <https://doi.org/10.1523/JNEUROSCI.2650-08.2008>
50. Harriott AM, Schwedt TJ (2014) Migraine is associated with altered processing of sensory stimuli. *Curr Pain Headache Rep* 18:458. <https://doi.org/10.1007/s11916-014-0458-8>
51. Zhuo Y, Wu Y, Xu Y et al (2017) Combined resting state functional magnetic resonance imaging and diffusion tensor imaging study in patients with idiopathic restless legs syndrome. *Sleep Med* 38:96–103. <https://doi.org/10.1016/j.sleep.2017.06.033>
52. Valfrè W, Rainero I, Bergui M et al (2008) Voxel-based morphometry reveals gray matter abnormalities in migraine. *Headache* 48:109–117. <https://doi.org/10.1111/j.1526-4610.2007.00723.x>
53. Schwedt TJ, Chong CD, Chiang CC et al (2014) Enhanced pain-induced activity of pain-processing regions in a case-control study of episodic migraine. *Cephalalgia* 34:947–958. <https://doi.org/10.1177/0333102414526069>
54. De Pauw R, Coppieters I, Caeyenberghs K et al (2019) Associations between brain morphology and motor performance in chronic neck pain: a whole-brain surface-based morphometry approach. *Hum Brain Mapp* 40:4266–4278. <https://doi.org/10.1002/hbm.24700>
55. Palermo S, Benedetti F, Costa T et al (2015) Pain anticipation: an activation likelihood estimation meta-analysis of brain imaging studies. *Hum Brain Mapp* 36:1648–1661. <https://doi.org/10.1002/hbm.22727>
56. Budell L, Kunz M, Jackson PL et al (2015) Mirroring pain in the brain: emotional expression versus motor imitation. *PLoS One* 10(2):e0107526. <https://doi.org/10.1371/journal.pone.0107526>
57. Ichesco E, Schmidt-Wilcke T, Bhavsar R et al (2014) Altered resting state connectivity of the insular cortex in individuals with fibromyalgia. *J Pain* 15:815–826. <https://doi.org/10.1016/j.jpain.2014.04.007>
58. Stoeter P, Bauermann T, Nickel R et al (2007) Cerebral activation in patients with somatoform pain disorder exposed to pain and stress: an fMRI study. *Neuroimage* 36:418–430. <https://doi.org/10.1016/j.neuroimage.2007.01.052>
59. Rocca MA, Messina R, Colombo B et al (2014) Structural brain MRI abnormalities in pediatric patients with migraine. *J Neurol* 261:350–357. <https://doi.org/10.1007/s00415-013-7201-y>
60. Magon S, May A, Stankewitz A et al (2015) Morphological abnormalities of thalamic subnuclei in migraine: a multicenter MRI study at 3 tesla. *J Neurosci* 35:13800–13806. <https://doi.org/10.1523/JNEUROSCI.2154-15.2015>
61. Li X, Chen L, Kuttan K et al (2019) Multi-atlas tool for automated segmentation of brain gray matter nuclei and quantification of their magnetic susceptibility. *Neuroimage* 191:337–349. <https://doi.org/10.1016/j.neuroimage.2019.02.016>
62. Ciampi E, Pareto D, Sastre-Garriga J et al (2017) Gray matter atrophy is associated with disability increase in natalizumab-treated patients. *Mult Scler* 23:556–566. <https://doi.org/10.1177/1352458516656808>
63. Lu CQ, Jiao Y, Meng XP et al (2018) Structural change of thalamus in cirrhotic patients with or without minimal hepatic encephalopathy and the relationship between thalamus volume and clinical indexes related to cirrhosis. *Neuroimage Clin* 20:800–807. <https://doi.org/10.1016/j.nicl.2018.09.015>
64. Coppola G, Petolicchio B, Di Renzo A et al (2017) Cerebral gray matter volume in patients with chronic migraine: correlations with clinical features. *J Headache Pain* 18:115. <https://doi.org/10.1186/s10194-017-0825-z>

Publisher's note Springer Nature remains neutral with regard to jurisdictional claims in published maps and institutional affiliations.